Journal of Inflammation Research

Dovepress
Taylor & Francis Group

Open Access Full Text Article

ORIGINAL RESEARCH

Immune Cell Characteristics in a Gut-Kidney Axis-Induced Mouse Model of IgA Nephropathy: The Upregulated Dendritic Cells and Neutrophils

Jiaqi Liu, Yuna Chen, Qijun Wan

Department of Nephrology, Shenzhen Second People's Hospital, The First Affiliated Hospital of Shenzhen University, Shenzhen, Guangdong, People's Republic of China

Correspondence: Qijun Wan, Department of Nephrology, Shenzhen Second People's Hospital, The First Affiliated Hospital of Shenzhen University, Shenzhen, 518035, People's Republic of China, Tel +86-755-83366388, Email yiyuan2224@sina.com

Background: IgA nephropathy (IgAN) is the leading type of primary glomerulonephritis, significantly contributing to chronic kidney disease (CKD) and renal failure. The pathogenesis of IgAN is the multi-hit hypothesis regarding overproduction and accumulation of galactose-deficient (Gd-IgA1). Recent findings have revealed gut microbiota dysbiosis and immune responses are essential in the development of IgAN, attracting increasing attention. This study aimed to map mucosal immune cells in IgAN influenced by gut microbiota, investigating the role of innate immune cells in kidney damage.

Methods: Fecal samples were acquired from both patients and controls for subsequent animal experiments. Mice received a broad-spectrum antibiotic cocktail to eliminate their intestinal microflora, followed by a gavage with fecal microbiota from clinical individuals. Murine intestinal and kidney tissues were collected for flow cytometry. Intestine and kidney histopathology, immunofluorescence, and inflammatory cytokine expression were assessed in the murine models. The mucosal epithelium's structure and function, along with the innate immune cell response, were analyzed.

Results: Mice exhibited the IgAN phenotype following colonization with gut microbiota from IgAN patients. These mice (IgAN-FMT mice) showed renal dysfunction and increased pathology of tissue injury in both intestine and kidneys. IgAN-FMT mice showed heightened pro-inflammatory cytokine (IL-6 and TNF-α) activity, greater antibody (IgA and complement C3) deposition and decreased expression of mucosal barrier protein (ZO-1, Occludin) compared to the control group. Furthermore, $CD11c^{+}$dendritic cells were more abundant in the murine intestine and kidneys compared to the control group.

Conclusion: The gut-kidney axis, including microbiota homeostasis and innate immune cell response, contributes to the pathogenesis of IgAN. Gut dysbiosis and hyperactivated immune cells like $CD11c^{+}$dendritic cells can affect the mucosal barrier and exacerbate the renal damage, being novel insights into immunotherapeutic strategies for IgAN.

Keywords: IgA nephropathy, fecal microbiota transplantation, gut microbiome, mucosal immunity, innate immune cells

Introduction

IgA nephropathy (IgAN) is the predominant type of primary glomerulonephritis and a major contributor to chronic kidney disease (CKD) and end-stage renal disease (ESRD).[1] Globally, 2.5 per 100,000 adults are diagnosed with IgAN annually.[2,3] Patients with IgAN confer a high risk of progressing to kidney failure over several years to decades.[1] Pathogenesis of IgAN proposes a "multi-hit" hypothesis:[4,5] It begins with the excessive production and accumulation of galactose-deficient IgA1 (Gd-IgA1). Subsequently, Gd-IgA1 leads to self-recognition and production of antibodies autoantibodies. Autoantibodies facilitate the formation and aggregation of immune complexes. Finally, immune complex is deposited in mesangial glomeruli, leading to renal inflammation and scarring.

Gut microflora has been reported to participate in multisystem diseases, especially immunological diseases including IgAN. Research indicates that gut microbiota dysbiosis can lead to mucosal damage, contributing to excessive Gd-IgA1 production.[6] Fecal microbiota transplantation (FMT) to correct microbiota disorder has been shown to markedly reduce

Received: 8 February 2025
Accepted: 11 June 2025
Published: 1 July 2025

Gd-IgA1 accumulation, mitigate albuminuria and ease glomerular inflammation in IgAN murine models.[7,8] The research on $\alpha1^{KI}$-$CD89^{Tg}$ mouse model demonstrated that transplanting fecal microbiota from IgAN patients exhibited increased serum levels of B cell activating factor (BAFF) and Gd-IgA1, leading to over-deposition of immune complexes in glomeruli, whereas microbiota from healthy donors relieved clinical symptoms.[7]

The interaction between the mucosal immune system and gut microbiota plays a pivotal role in maintaining intestinal homeostasis. Within gut-associated lymphoid tissue (GALT), innate immune cells in Peyer's patches recognize microbial signals via Toll-like receptors (TLRs).[9] Subsequently, antigen-presenting cells (APCs) process and transmit these signals to effector cells, stimulating cells differentiation, IgA class switching and autoantibodies synthesis.[10] However, the relationship between the mucosal immune response and IgAN has not been fully clarified. The impact of gut microbiota on mucosal innate immune cells involved in IgAN progression remains unclear.

Although routine treatment (including supportive care and immunosuppressive therapies) for IgAN has been applied in clinical practice for decades, its long-term benefits are still under debate.[11] In recent years, scientists have gradually developed great interest in revealing the immune mechanism and investigating mucosal immunization for effective IgAN therapy, aiming to discover novel therapeutic targets. Our study aimed to enhance understanding of the IgAN mechanism by modeling mice with FMT from patients, focusing on mucosal response changes in disease to explore the interaction between gut microbiota and mucosal innate immunity.

Materials and Methods

Study Design

The Human Research Ethics Committee of the First Affiliated Hospital of Shenzhen University, Shenzhen, China (No.2024SYY-025) approved this study, which adhered to the Declaration of Helsinki. Consent was secured from all study individuals. Participants were selected from the First Affiliated Hospital of Shenzhen University between December 2023 and September 2024. Only participants aged between 18 and 60 years were included. To eliminate the influence of medications and hospital-related factors on gut microbiota, we exclusively selected samples from newly diagnosed IgAN patients who had not received treatment or medication prior to admission. Inclusion criteria required a renal biopsy confirming IgAN and an estimated GFR (eGFR) of at least 60 mL/min/1.73m^2. Five patients with biopsy-confirmed idiopathic membranous nephropathy (MN) were included as a disease control (DC). The healthy control group consisted of five healthy participants selected from the same hospital's physical examination center at identical time points. The patients were all Han Chinese from Guangdong, residing in the same geographic region, and had alike food preferences. Exclusion criteria included immunosuppression or kidney transplant, use of oral antibiotics, probiotics, prebiotics, or synthetic bacteria within two months, history of cancer, hematological disorders, inflammatory bowel disease (IBD), or other severe gastrointestinal conditions, and women who are pregnant, recently pregnant, or lactating. Exclusion criteria for IgAN add secondary IgA deposits associated with conditions such as rheumatoid arthritis, systemic lupus erythematosus, hepatitis-related glomerulonephritis, Henoch-Schönlein purpura, and kidney transplantation. In the Supplementary Table 1 and Supplementary Figure 1, you can find clinical details for patients with IgAN, DC, and HC.

Mouse Model

Mice euthanized after the last gavage was completed and examined for further analysis. The Institutional Animal Care and Use Committee of Shenzhen Second People's Hospital approved the mouse experiments (No.20240047). The experiments adhered to the Laboratory Animal Science Association guidelines. The committee's rules were complied with in the experiments. Eight-week-old wild-type male C57BL/6j mice were obtained from Jackson Laboratory. Mice were kept in a pathogen-free environment, with each ventilated cage containing aspen bedding and housing 4 to 5 mice. The cycle consisted of 12 hours of light and 12 hours of darkness, sustained at standard room temperature and humidity.

Rodent chow and water were available to the mice at all times. Following a 1-week adaptation period, the mice were given a daily oral dose of a broad-spectrum antibiotic cocktail (ABX) for 7 days to eliminate the initial gut microbiome. The cocktail included vancomycin (100 mg/kg), neomycin sulfate (200 mg/kg), ampicillin (200 mg/kg), and metronidazole (100 mg/kg). The FMT procedure followed established protocols.[12] Fresh fecal samples from each individual

were rapidly combined with an equal volume of PBS containing 25% glycerol and then frozen with liquid nitrogen. The samples were stored at −80°C until required. The feces (100 mg resuspended in 1 mL PBS) were processed as standard procedure and fabricated into transplant supernatant. Over the course of 8 weeks, 200 μL of pooled transplant material from donors in each group (IgAN, DC and HC) was administered to each recipient mouse by gavage three times weekly. After the final gavage, the mice were euthanized and examined for further study.

Isolation of Intestinal and Kidney Cells

Single-cell homogenates were prepared according to standard protocols. The tissues were harvested by perfusion with PBS. Kidney tissues were sectioned into small pieces and incubated in a digestion buffer at room temperature with shaking at 200 rpm for 30 to 45 minutes. The kidney digestion solution comprised 0.05% dispase and 0.1% Type II Collagenase in RPMI-1640 supplemented with 2% FBS. After digestion, the cell suspensions were filtered through 70 μm strainers, centrifuged, and resuspended in PBS.

The intestines were cleaned, and their contents were flushed with PBS. After removing the fat, the intestines were inverted and cut into segments measuring 0.5 to 1 cm. Next, the intestinal tissues were placed in an extraction buffer and incubated at ambient temperature in shaker, rotating at 200 rpm for a duration of 15 minutes. The buffer used for extraction contains 1 mM DTT and 5 mM EDTA, mixed in RPMI-1640 with 2% FBS. Subsequently, the leftover tissues were rinsed with PBS, chopped, and placed in a digestion buffer for incubation, shaking at 200 rpm (at ambient temperature) for 30 to 45 minutes. The homogenates, after being liberated through digestion, were filtered and resuspended in PBS to produce the single-cell suspensions.

Flow Cytometry Analysis

Flow cytometric analysis was performed according to standard protocols. Single-cell suspensions of the kidney and intestine were blocked with FcBlock (BD Biosciences) and immunostained for further analysis using flow cytometry. The single-cell suspensions were stained with specific antibodies in the dark at 4°C for 30 minutes. Then the suspensions underwent a washing process followed by centrifugation at 500g for 5 minutes at 4 °C. The antibodies utilized are detailed in the Supplementary Table 2. Samples were collected using DxP Athena™ (Cytek Biosciences) and analyzed with FlowJo version 10 software.

Histological Examination and Glycogen PAS Stain

Intestinal and renal samples were treated with formaldehyde and encased in paraffin. After dewaxing, 2–4 μm thick sections were stained with hematoxylin and eosin (HE) following the standard protocol. Inflammation severity in the small and large intestines was assessed according to the method outlined in Supplementary Table 3.[13] The scores of inflammation severity were summed to yield a total histological score ranging from 0 (no change) to 9 (extensive inflammation and tissue damage).

Kidney tissues were collected for periodic acid-Schiff (PAS) staining according to standard laboratory procedures. The tissues were sliced into 3 μm thick sections and stained using PAS. A quantitative analysis assessed the percentage of glomeruli exhibiting segmental and global sclerosis, mesangial cell proliferation, or increased mesangial matrix. Each sample received a semi-quantitative score based on the percentage of affected glomeruli (0: 0%; 1: 1–24%; 2: 25–49%; 3: >50% of 20 glomeruli) as previously described.[14]

Immunofluorescence Staining

For the immunofluorescence experiments, kidney tissues were collected immediately after the mice were sacrificed. Sections of frozen tissue, 5 μm thick, were blocked using a perm/blocking buffer. The perm/blocking buffer consists of 0.2% Triton X-100 and 10% donkey serum in PBS. At 4°C, sections were stained overnight, either on their own or with antibodies against FITC-labeled goat anti-mouse IgA (ab97234, Abcam) or rat anti-mouse C3 (ab11862, Abcam). After washing, the sections were incubated for one hour with the appropriate secondary immunofluorescent antibody.4′-6′-diamidino-2-phenylindole (DAPI) was applied to stain the nuclei. The labeled sections were examined using either

a Zeiss LSM 880 confocal fluorescence microscope or the PerkinElmer Mantra System (USA). Mean fluorescence intensity (MFI) was calculated using ImageJ software.

ELISA, Biochemical Tests

Serum samples were collected from each mouse at the conclusion of the experiments. Serum IgA antibodies were measured using an ELISA kit from Cusabio Biotech, following the manufacturer's instructions. A fully automatic biochemical detector (Chemray 240; Rayto, China) was used to measure serum creatinine (SCR) and blood urea nitrogen (BUN) levels.

Total RNA Isolation and Reverse Transcription

The intestinal and kidney tissues were manually homogenized using a homogenizer and processed for RNA isolation. Total RNA was extracted using the RNeasy Mini Kit (Qiagen, 74106) following the manufacturer's instructions. Using Nanodrop, the concentration and purity of RNA were evaluated. RNA was transcribed into cDNA using the High-Capacity cDNA Reverse Transcription Kit (Applied Biosystems), following the manufacturer's instructions.

RT-qPCR (Reverse Transcription-Quantitative Polymerase Chain Reaction)

The cDNA nucleotide sequences of IL-6, TNF-α, ZO-1, Occludin and GAPDH genes were acquired from the National Center for Biotechnology Information database (https://www.ncbi.nlm.nih.gov/). Primers for each gene were designed via PrimerBank (https://pga.mgh.harvard.edu/primerbank/) and validated using Primer-BLAST (https://www.ncbi.nlm.nih.gov/tools/primer-blast/). Quantitative reverse transcription PCR (qRT-PCR) was conducted with SYBR Green Master Mix (Roche) on a QuantStudio™ 7 Flex Real-Time PCR instrument (Applied Biosystems) following the manufacturer's guidelines. Instrument model was set under conditions: at 50 °C for 2 min and 95 °C for 10 min, and then at 95 °C for 15s and 60 °C for 1 min as 1 cycle for 40 times in total. Then, melting curve reaction was conducted under conditions: at 95 °C for 15s, 60 °C for 1 min, 95 °C for 15s, 60 °C for 15s, 1 cycle for once. Target gene expression was normalized to the housekeeping gene GAPDH and expressed as $2^{-\Delta CT}$, with fold change calculated as $2^{-\Delta\Delta CT}$ relative to the control group. The primers utilized are detailed in Supplementary Table 4.

Statistical Analysis

Data are displayed as mean ± SEM, except where noted otherwise. Figure legends provide details on each experiment's sample size (n), probability (p) values, and associated statistical tests. All experiments were replicated multiple times with independent animals. GraphPad Prism facilitated the analysis and plotting of the data. Shapiro–Wilk Normality test was used to assess normality. Statistical analyses employed Student's t-test and one-way ANOVA with Tukey's multiple comparison test, as appropriate. Tukey and Dunnett's multiple comparison tests were applied as appropriate. All data were analyzed using two-tailed tests. Statistical significance was determined using a P-value threshold of 0.05. P values are depicted as follows: **** $P < 0.0001$, *** $P < 0.001$, ** $P < 0.01$, * $P < 0.05$.

Results

Humanized Microbiota-Colonized Mice Displayed the Presenting Features of IgAN

To elucidate whether gut microbiome has a direct impact on IgAN, fresh fecal samples from clinical patients and healthy individuals were collected for further experiments. A broad-spectrum antibiotic cocktail (ABX) was given to C57BL/6 mice to diminish their intestinal microbiota. Fecal bacteria from patients with IgAN were transplanted into mice. Mice were gavaged with FMT from both MN patients and healthy controls as a control group. Figure 1A illustrates the experimental design schematic for the mouse study. Antibiotic treatment led to a decrease in body weight in recipients (Figure 1B). The recipients then adapted to the FMT and gained weight during the course of the experiment (Figure 1B). The IgAN-FMT (IgA nephropathy fecal microbiota transplantation) group showed the greatest increase of serum creatine (SCR) and blood urea nitrogen (BUN) among the three groups (Figure 1C and D). Serum IgA was also estimated, and Figure 1E shows the highest abundance of IgA from group of IgAN-FMT compared to that in DC-FMT and HC-FMT.

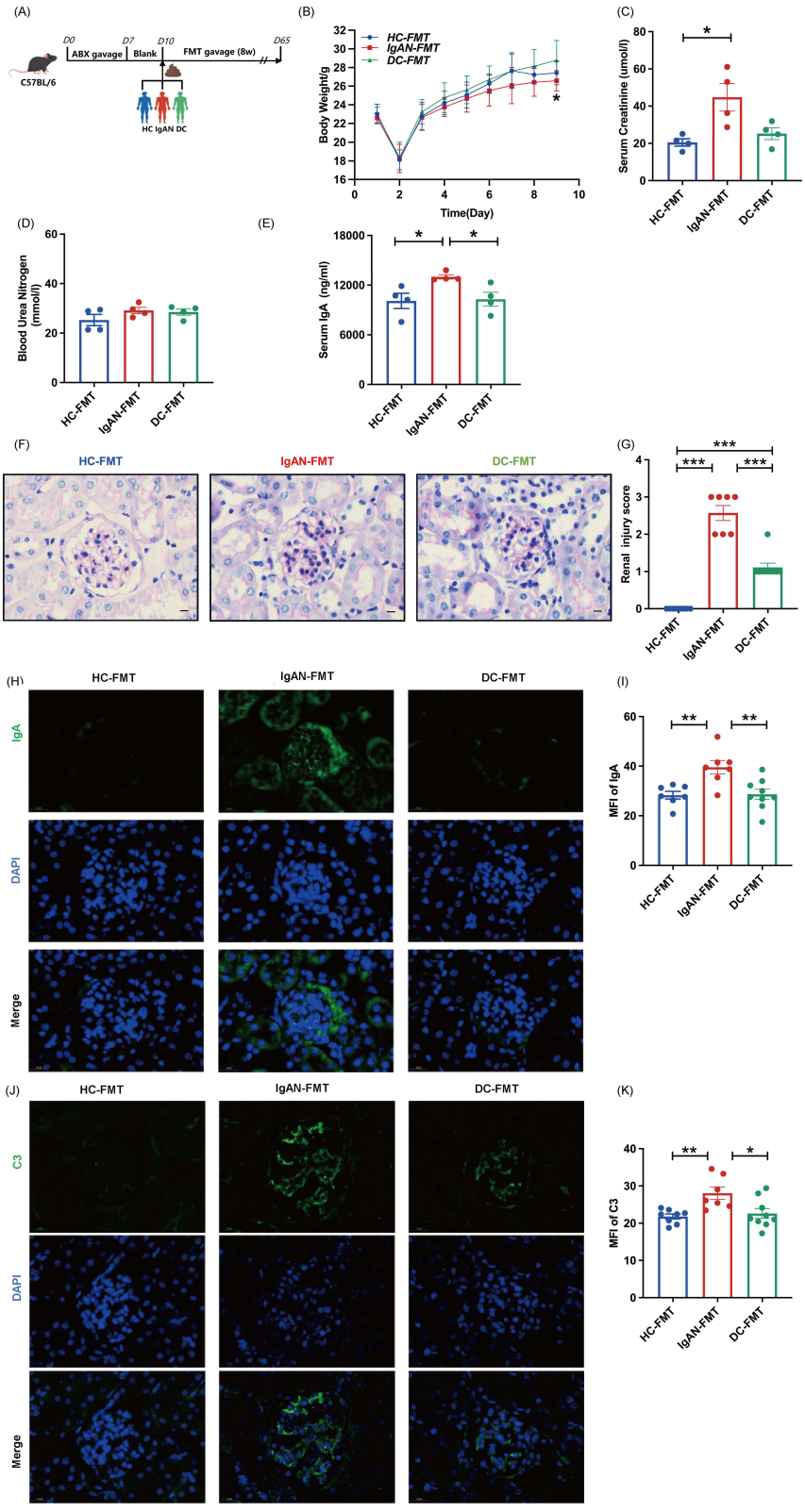

Figure 1 Humanized microbiota-colonized mice displayed the presenting features of disease like IgAN. (**A**) Schematic of experimental design of mice. (**B**) The time-course changes of body weight in mice. (**C** and **D**) Estimation of kidney function indicators: (**C**) Serum creatine and (**D**) blood urea nitrogen. (**E**) Detection of serum IgA in mice. (**F** and **G**) Representative images of Periodic acid-Schiff (PAS)-stained kidney sections. Pathological injury score was analyzed (n = 7–9 per group). Scale bars, 20 μm. (**H** and **I**) Representative images of IgA (green) deposition in the glomeruli. Mean fluorescence intensity (MFI) of IgA was calculated by ImageJ (n = 7–9 per group). Scale bars, 20 μm. (**J** and **K**) Representative images of C3 (green) deposition in the glomeruli. Mean fluorescence intensity (MFI) of C3 was calculated by ImageJ (n = 7–9 per group). Scale bars, 20 μm. Data are presented as the mean ± SEM. One-way ANOVA tests (**B–E, I**, and **K**) were performed. ***$P < 0.001$; **$P < 0.01$; *$P < 0.05$.

https://doi.org/10.2147/JIR.S519521

To further evaluate damage of the kidney, we undertook PAS staining of kidney tissue and obtained pathological renal injury scores according to standard procedures.[14] In the IgAN-FMT mouse group, there was a significant increase in mesangial proliferation and mesangial matrix expansion (Figure 1F and G). Immunofluorescence tests were conducted to discover the usual deposition of IgA and complement C3 immune complexes in glomeruli. MFI measurements showed increased intensities of both IgA and C3 in IgAN-FMT mice compared to other groups (Figure 1H–K). These results demonstrate that transplantation of intestinal bacteria from IgAN patients causes mice to behave like IgAN.

Gut Microbiome Induced Intestinal Barrier Disruption and Immune Activation

Using hematoxylin–eosin (HE) staining to analyze mucosal barrier injury, we found that IgAN-FMT mice exhibited aggravated injury to the ileum and colon (Figure 2A and B). Intestinal damage manifests as greatly shortened villi, reduced goblet cells, damaged epithelium, and increased infiltration of inflammatory cells. Histopathological analysis showed the higher villous height-to-crypt depth ratio (Figure 2C) and histological injury score (Figure 2D and E) in IgAN-FMT recipient.

The expression of inflammatory cytokines was examined using quantitative reverse transcription PCR (qRT-PCR) to analyze proinflammatory cytokines and mucosal protein transcripts in the intestine. Mice receiving fecal bacteria from IgAN patients exhibited elevated IL-6 and TNF-α expression compared to control groups (Figure 2F). And the reduction in ZO-1 and Occludin levels in the gut indicates a compromised mucosal barrier function (Figure 2G).

To determine the features of the antibody-related immune cells, intestinal tissue was collected to prepare single-cell suspensions for flow techniques. Figure 2H presents flow cytometric plots of B lymphocytes (B cells), specifically gated on $B220^+$ cells. The proportion of B cells was not significantly different among the IgAN-FMT, HC-FMT, and DC-FMT mice (Figure 2I). Furthermore, we examined a subset of $B220^+CD38^+$ cells and found similar proportions among these groups (Figure 2J and K). Considering that the expression of antibody IgA may represent the function of B cells, we also performed immunostaining for IgA in intestinal single-cell flow cytometric analysis (Figure 2L). The percentage of $B220^+CD38^+IgA^+$ cells in lymphocytes was higher than that in HC-FMT mice, and there was no difference when compared with DC-FMT mice (Figure 2M).

Pro-Inflammatory Activation of Immune Cells in the Kidney

Flow cytometry was employed to examine the features of the antibody-related immune cells in renal tissues. The percentage of $B220^+$ cells was higher in IgAN-FMT mice than that in HC-FMT mice. No statistical significance was detected when compared to DC-FMT mice (Figure 3A and B). The percentage of $B220^+CD38^+$ cells exceeded that of the control group (Figure 3C and D). When stained with IgA, the proportion of IgA^+ cells within lymphocytes in IgAN-FMT mice was higher than that in HC-FMT and DC-FMT mice (Figure 3E and F).

In addition, we evaluated the inflammatory environment using qRT-PCR. Interleukin-6 (IL-6) and tumor necrosis factor-α (TNF-α) expression levels were elevated in the kidneys of IgAN-FMT mice compared to control groups (Figure 3G and H). Using DC-FMT mice as controls showed no significant differences.

Innate Immune Cells Profile in Intestine in Humanized Microbiota-Colonized Mice

To map profile of innate immune cell in the intestine, innate immune cells were identified and examined using flow cytometry. The process of identification was grounded in a collection of well-recognized markers.[15] The gating strategy of flow cytometry is presented in Figure 4A.

Statistical analysis of innate immune cell proportions revealed a significant increase in the proportion of DC within lymphocytes in the intestinal tissue of IgAN-FMT mice compared to control groups (Figure 4D and F). Flow cytometry analysis showed no variation in the percentages of neutrophils, macrophages, or monocytes, as depicted in Figure 4B–E, G and H. When gated on $Ly6C^+$lymphocytes, there was a critical difference between disease group compared to HC-FMT group (Figure 4I and J).

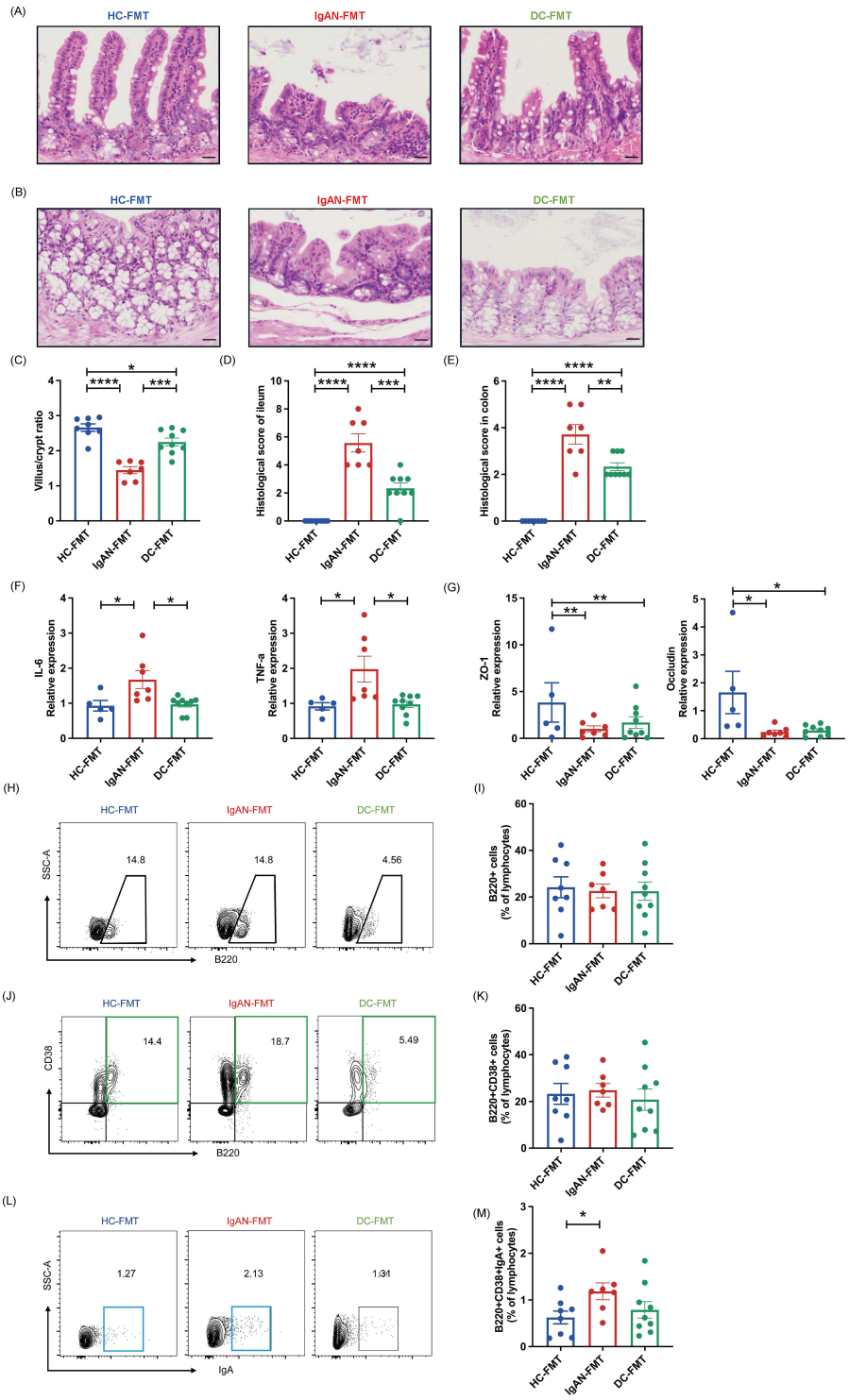

Figure 2 Gut microbiome induced intestinal barrier disruption and immune activation. (**A**) Representative images of Haematoxylin–Eosin (HE)-stained ileum sections in mice. Scale bars, 50 μm. (**B**) Representative images of HE-stained colon sections. Scale bars, 50 μm. (**C**) The ratio of villous height-to-crypt depth in HE-stained sections was analyzed. (**D**) Histological score in ileum was analyzed. (**E**) Histological score of HE-stained colon sections was analyzed. (**F**) Real-time PCR analysis of pro-inflammatory cytokines IL-6 and TNF-α transcript in intestine was performed (n = 5–9 per group). (**G**) Real-time PCR analysis of mucosa barrier proteins ZO-1 and Occludin transcript in intestine was performed (n = 5–9 per group). (**H** and **I**) Representative flow cytometry plots and statistical data showing the percentage of B cells ($B220^+$) within lymphocytes in intestine tissues. B cells: B lymphocytes. (**J** and **K**) Representative flow cytometry plots and statistical data showing the percentage of $B220^+$ $CD38^+$ subsets in lymphocytes in intestine tissues. (**L** and **M**) Representative flow cytometry plots and statistical data showing the percentage of $B220^+$ $CD38^+$ IgA^+ cells in lymphocytes in intestine tissues. Data are presented as the mean ± SEM. N = 7–9 per group, except where noted otherwise. One-way ANOVA test (**B** and **E**–**G**). $^{****}P < 0.0001$; $^{***}P < 0.001$; $^{**}P < 0.01$; $^{*}P < 0.05$.

https://doi.org/10.2147/JIR.S519521

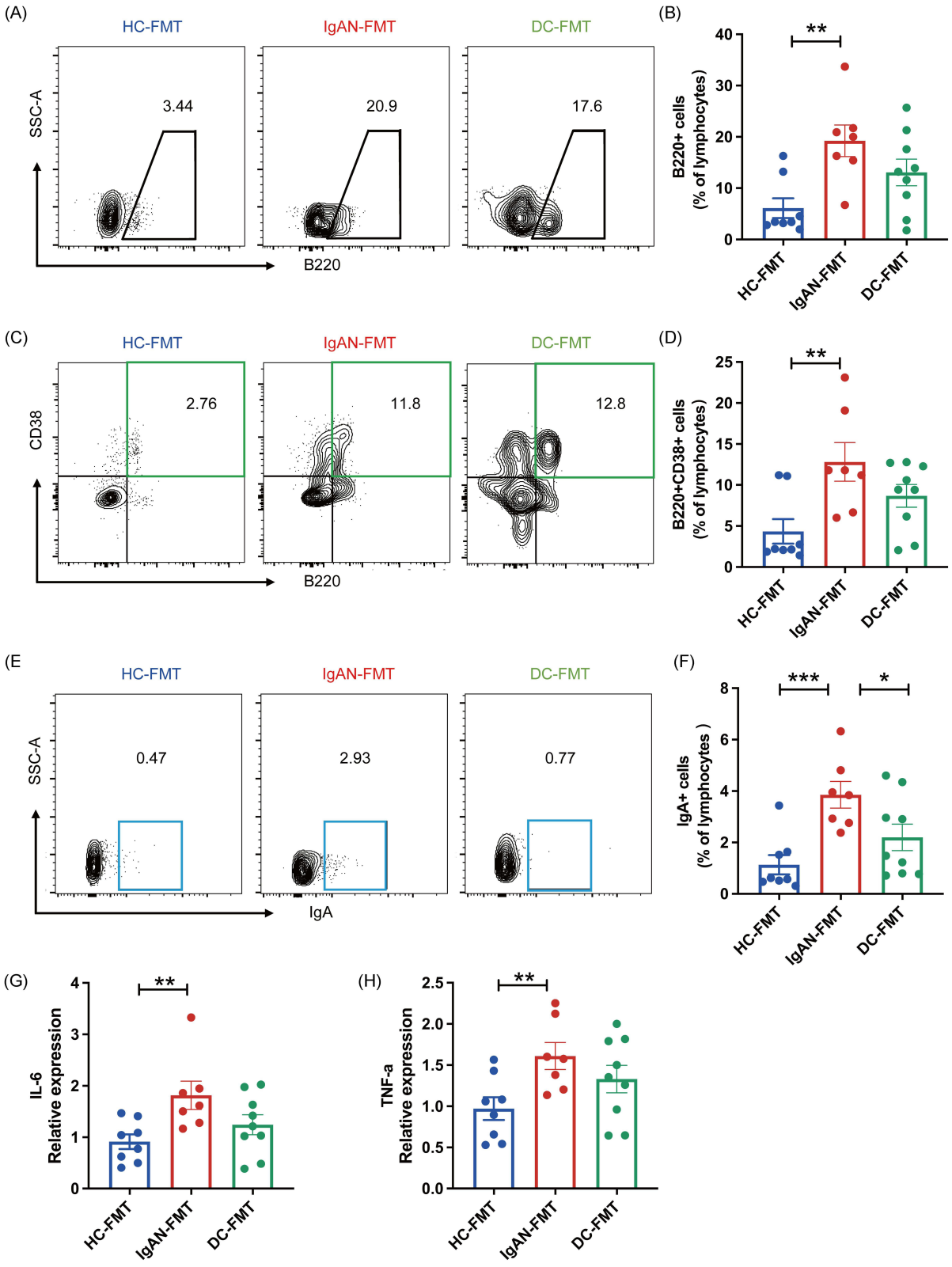

Figure 3 Immune cells and pro-inflammatory activation in kidney. (**A** and **B**) Representative flow cytometry plots and statistical data showing the percentage of B cells ($B220^+$) within lymphocytes in renal tissues. (**C** and **D**) Representative flow cytometry plots and statistical data showing the percentage of $B220^+$ $CD38^+$ B cells in lymphocytes in renal tissues. (**E** and **F**) Representative flow cytometry plots and statistical data showing the percentage of IgA^+ cells within lymphocytes in renal tissues. (**G-H**) Real-time PCR analysis of pro-inflammatory cytokines IL-6 and TNF-α transcript in kidney was performed. ***$P < 0.001$; **$P < 0.01$; *$P < 0.05$.

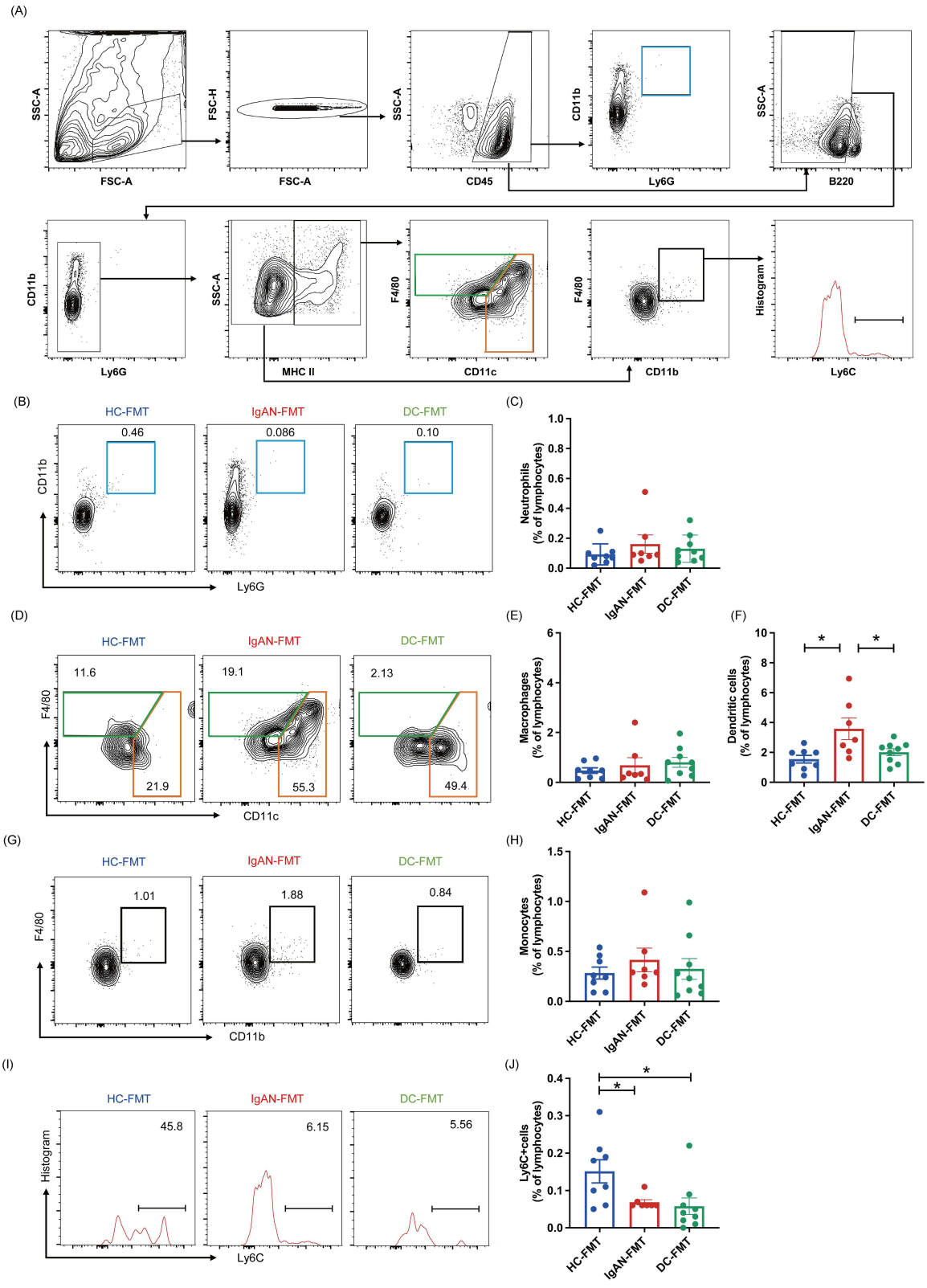

Figure 4 Innate immune cells profile in intestine in humanized microbiota-colonized mice. (**A**) Gating strategy used to identify innate immune cells of Analysis of neutrophils ($CD45^+$ $CD11b^+$ $Ly6G^+$), macrophages ($CD45^+$ $MHCII^+$ $F4/80^+$ $CD11c^{lo}$), dendritic cells (DC) ($CD45^+$ $MHCII^+$ $F4/80^{lo}$ $CD11c^{hi}$), and monocytes ($CD45^+$ $MHCII^-$ $CD11b^+$ $F4/80^+$ $Ly6C^{+/-}$) in intestine. (**B** and **C**) Representative flow cytometry plots and statistical data showing the percentage of neutrophils within lymphocytes in mice. (**D**–**F**) Representative flow cytometry plots and statistical data showing the percentage of macrophages and DC in lymphocytes in mice. (**G** and **H**) Representative flow cytometry plots and statistical data showing the percentage of monocytes within lymphocytes in mice. (**I** and **J**) Representative flow cytometry plots and statistical data showing the percentage of $Ly6C^+$ monocytes in lymphocytes in mice. Data are presented as the mean ± SEM. N = 7–9 per group One-way analysis of variance (ANOVA) was performed. *$P < 0.05$.

https://doi.org/10.2147/JIR.S519521

Profile of Innate Immune Cells in Kidneys of Mice Colonized with Humanized Microbiota

To outline the innate immune profile in kidney, we identified innate immune cells in the kidneys of these mouse models. A representative gating strategy for the flow cytometric analysis is shown in Figure 5A. We found that IgAN-FMT recipients showed a higher proportion of neutrophils compared to control recipients in kidney tissue (Figure 5B and C). The IgAN-FMT mice exhibited a significantly higher proportion of DC within lymphocytes compared to the HC-FMT and DC-FMT mice (Figure 5D and F). Flow cytometry analysis revealed no significant differences in the percentages of macrophages (Figure 5D and E), monocytes (Figure 5G and H), or Ly6C^{+}lymphocytes (Figure 5I and J).

Discussion

Scientists have described alterations in the intestinal and oropharyngeal microbial composition in IgAN patients from different populations, including Italy, Canada, and Han Chinese—compared to healthy controls.[16–19] A clinical cohort reported that the alteration of Escherichia-Shigella mostly contributes to microbial dysbiosis in patients with IgAN.[20] Notably, newly investigation indicated that IgAN patients had a higher relative abundance of mucin-degrading bacteria, *Akkermansia muciniphila*, compared to HC or CKD patients.[6] Furthermore, researchers have demonstrated that recolonization of A. *muciniphila* in $\alpha1^{KI}$-$CD89^{Tg}$ mice developed a progressive IgAN phenotype.[6] Another research depicted that the oral commensal bacteria C42 promoted production of IgA in gddY mice.[21] Mechanistically, gut microbiota disorders could stimulate the overproduction of Gd-IgA1 through TLR4/MyD88/NF-κB pathway and BAFF/APRIL in mice.[14] These findings together suggest that the mucosal microbiome is crucial in human diseases by influencing host mucosal defense and humoral immune responses.[22] In our study, we demonstrated the transplantation of fecal microbiota from patients with IgAN induced renal injury in mice, with histological damage and immune complexes deposition. Furthermore, both intestinal and renal innate immune cells were influenced by the specific gut microbiota of IgAN, implying the interaction between gut microbiome and mucosal immunity in the disease.

Mucosal immune response plays a key part in pathophysiology of IgAN. Genome-wide association studies (GWAS) have identified the susceptibility loci of IgAN (eg DEFA, TNFSF13, and ITGAM-ITGAX), which encoded proteins that maintaining the intestinal barrier and regulating mucosal immune network.[23,24] In clinical study, the intestinal histology of IgAN patients described the atrophy with elongated crypts and shortened villous length.[25,26] On the experimental side, pathogenic IgA1 is transported from mucosal sites into the circulation and ultimately deposits in the kidney.[1,6] Emerging findings demonstrated that the damage index of intestinal barrier function like D-LAC, sICAM-1 and LPS were increased in mice after transplantation fecal bacteria from IgAN patients compared with those from HC.[14] In our research, we similarly observed the disruption of intestinal mucosa and the decreased barrier function accompanied by kidney injury in the IgAN recipient. These accumulating data imply that mucosal immune response is implicated in the onset and mechanism of IgAN, proving the existence of a mucosa-kidney axis or gut-kidney axis.[26]

Emerging evidence have proposed that the production of pathogenic Gd-IgA1 may result from overactivation of the intestinal environment.[6,27] Recently, experts revealed a pivotal and unique role of innate immune cells in hyperresponsive mucosal immunity: The innate immune cells not only changed under the stimulation of pathogen but also over-activated when encountered stimulation again, showing more amplified responses upon secondary stimulation compared to primary challenges.[28] These hyperresponsive innate immune cells increase non-specific responses to subsequent infections and improve survival.[29] In the intestinal mucosa, APC process antigens and stimulate the differentiation, proliferation, and IgA secretion in B cells.[30] Interleukins like IL-6 is also critical in activating effector cells to produce antibodies.[31] It is worth noting that APC including dendritic cells and macrophages presented overexpression in IgAN patients, indicating the activation of the immune system.[30,32] In patients with IgAN, elevated level of monocyte-macrophages was noticed in the duodenal mucosa.[33] Importantly, the degree of intestinal inflammation is associated with serum IgA levels, proteinuria, and hematuria.[34] Consistent with previous research, we found a dominant expansion of CD11c^{+}dendritic cells in the intestine and kidney. In our experiments, elevated IL-6 and TNF-α levels were also observed in IgAN-FMT mice compared to control groups, indicating enhanced immune activation. Modulation of innate

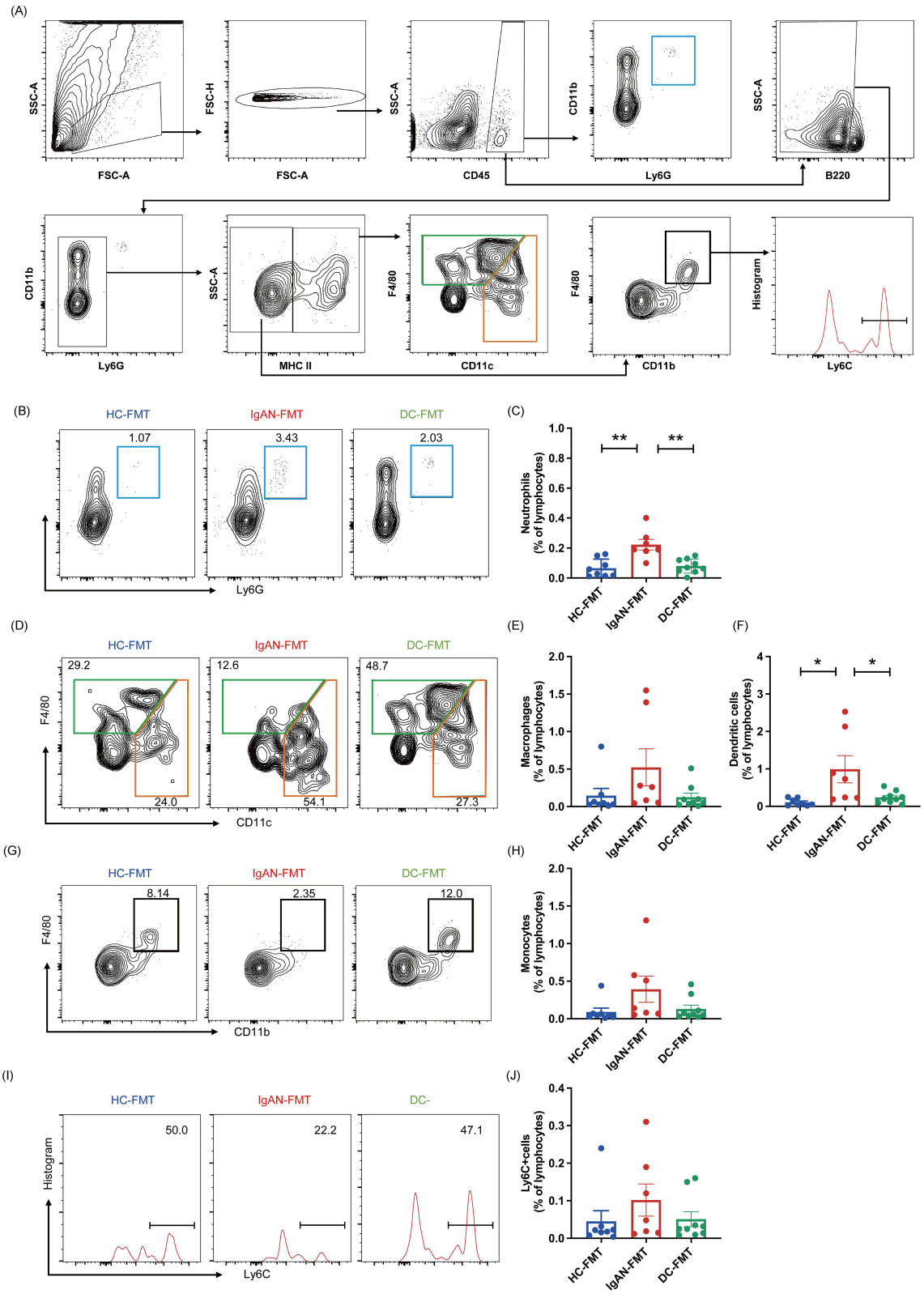

Figure 5 Innate immune cells profile in kidney in humanized microbiota-colonized mice. (**A**) Gating strategy used to identify innate immune cells of analysis in kidney. (**B** and **C**) Representative flow cytometry plots and statistical data showing the percentage of neutrophils in lymphocytes in mice. (**D**–**F**) Representative flow cytometry plots and statistical data showing the percentage of macrophages and DC within lymphocytes in mice. (**G** and **H**) Representative flow cytometry plots and statistical data showing the percentage of monocytes in lymphocytes in mice. (**I** and **J**) Representative flow cytometry plots and statistical data showing the percentage of Ly6C^{+} monocytes within lymphocytes in mice. Data are presented as the mean ± SEM. N = 7–9 per group One-way analysis of variance (ANOVA) was performed. $^{**}P < 0.01$; $^{*}P < 0.05$.

https://doi.org/10.2147/JIR.S519521

immune cells, as a newly intervention in oncology and autoimmune diseases, has attracted notable attention for its distinct advantages such as rapid, non-specific, and synergistic potential.[35,36]

Experts gradually developed great interest in investigating modulation of mucosal immunity or immune cells in IgAN, looking for mucosal immunization to effective IgAN therapy. A new therapeutic method has been created to administer an ileum-targeted release formulation of budesonide (TRF budesonide, Nefecon™) aimed at locally suppressing immune hyperactivity. Clinical studies by Nefecon suggested that Nefecon treatment significantly reduced urine albumin secretion and better preserved the eGFR.[37–39] Compared to placebo, Nefecon considerably prolonged the time to a confirmed 30% decrease in eGFR or kidney failure from baseline.[39] These results together offer mucosal immunization a promising future for clinical translation.

A major strength of our study is that we explored the gut-kidney axis implicated in the pathogenesis of IgAN, highlighting the importance of mucosal immunity in IgAN. Due to the absence of an academically recognized IgAN animal model, we employed IgAN humanized microbiota-colonized mice to investigate changes in the immune response. The limitations of present study include (1) lacking multiple models to validate the findings in our study and (2) insufficient manipulation of relevant innate immune cells like dendritic cells and molecular targets, thereby the mechanism underlying the involvement of these immune cells remains unclear. Future studies will focus on addressing these aspects to establish definitive causal relationships through specific pathway modulation. It is suggested that regulating APC like dendritic cells may be useful for immunotargeted therapy. While more basic and clinical research are required to solid this expectation.

Conclusions

Our findings showed that IgAN-FMT recipients had a strong propensity to form IgAN manifestations, performing related disruption of the intestinal barrier and expansion of $CD11c^{+}$dendritic cells in the disease. These results provide new insights into potential treatment targets, like modulating dendritic cells.

Abbreviations

IgAN, IgA nephropathy; CKD, Chronic kidney disease; Gd-IgA1, Galactose-deficient IgA1; ESRD, End-stage renal disease; FMT, fecal microbiota transplantation; ABX, antibiotics; BAFF, B cell activating factor; GALT, Gut-associated lymphoid tissue; APC, antigen-presenting cells; eGFR, estimated glomerular filtration rate; TLRs, Toll-like receptors; MN, membranous nephropathy; DC, disease control; HC, healthy control; HE, haematoxylin–eosin; PAS, periodic acid-Schiff; DAPI, 4′,6-diamidino-2-phenylindole; RT-qPCR, Reverse Transcription-Quantitative Polymerase Chain Reaction; ANOVA, one-way analysis of variance; BUN, blood urea nitrogen; SCR, serum creatine; MFI, Mean fluorescence intensity; B cells, B lymphocytes; GWAS, Genome-wide association studies.

Data Sharing Statement

The study's data are unavailable to the public due to privacy concerns for research participants. The corresponding author will provide the data supporting this article upon reasonable request.

Ethics Approval and Informed Consent

The study adhered to the Declaration of Helsinki and received approval from the Medical Ethics Committee of Shenzhen Second People's Hospital (ethics approval No. 2024SYY-025; animal ethics ID 20240047).

Informed consent was obtained in writing from all participants at enrollment for our human subjects' research, as detailed in the Methods section.

Consent for Publication

All participants signed a document of consent to publish.

Acknowledgments

We appreciate the participation of all patients. We thank all members of the Wan Laboratory for their fruitful discussions, support, and critical review of the manuscript. We thank the professors of the Department of Nephrology in Shenzhen for their constructive comments on research improvements. We express our gratitude to the patients and volunteers for their participation.

Author Contributions

All authors made a significant contribution to the work reported, whether that is in the conception, study design, execution, acquisition of data, analysis and interpretation, or in all these areas; took part in drafting, revising or critically reviewing the article; gave final approval of the version to be published; have agreed on the journal to which the article has been submitted; and agree to be accountable for all aspects of the work.

Funding

This research received support from The Second People's Hospital of Shenzhen, The First Affiliated Hospital of Shenzhen University, and was funded by the Shenzhen Key Medical Discipline Construction Fund (SZXK009), the Sanming Project of Medicine in Shenzhen (SZSM202211013), and the Guangzhou Science and Technology Project (202206080010).

Disclosure

The authors declare no conflicts of interest related to this study.

References

1. Cheung CK, Alexander S, Reich HN, Selvaskandan H, Zhang H, Barratt J. The pathogenesis of IgA nephropathy and implications for treatment. *Nat Rev Nephrol*. 2025;21(1):9–23. doi:10.1038/s41581-024-00885-3
2. McGrogan A, Franssen CF, de Vries CS. The incidence of primary glomerulonephritis worldwide: a systematic review of the literature. *Nephrol Dial Transplant*. 2011;26(2):414–430. doi:10.1093/ndt/gfq665
3. Willey CJ, Coppo R, Schaefer F, Mizerska-Wasiak M, Mathur M, Schultz MJ. The incidence and prevalence of IgA nephropathy in Europe. *Nephrol Dial Transplant*. 2023;38(10):2340–2349. doi:10.1093/ndt/gfad082
4. Suzuki H, Kiryluk K, Novak J, et al. The pathophysiology of IgA nephropathy. *J Am Soc Nephrol*. 2011;22(10):1795–1803. doi:10.1681/ASN.2011050464
5. Scionti K, Molyneux K, Selvaskandan H, Barratt J, Cheung CK. New insights into the pathogenesis and treatment strategies in IgA nephropathy. *Glomerular Dis*. 2022;2(1):15–29. doi:10.1159/000519973
6. Gleeson PJ, Benech N, Chemouny J, et al. The gut microbiota posttranslationally modifies IgA1 in autoimmune glomerulonephritis. *Sci Transl Med*. 2024;16(740):eadl6149. doi:10.1126/scitranslmed.adl6149
7. Lauriero G, Abbad L, Vacca M, et al. Fecal microbiota transplantation modulates renal phenotype in the humanized mouse model of IgA nephropathy. *Front Immunol*. 2021;12:694787. doi:10.3389/fimmu.2021.694787
8. Zhi W, Li A, Wang Q, et al. Safety and efficacy assessment of fecal microbiota transplantation as an adjunctive treatment for IgA nephropathy: an exploratory clinical trial. *Sci Rep*. 2024;14(1):22935. doi:10.1038/s41598-024-74171-4
9. Ye YL, Chuang YH, Chiang BL. Strategies of mucosal immunotherapy for allergic diseases. *Cell Mol Immunol*. 2011;8(6):453–461. doi:10.1038/cmi.2011.17
10. Bemark M, Pitcher MJ, Dionisi C, Spencer J. Gut-associated lymphoid tissue: a microbiota-driven hub of B cell immunity. *Trends Immunol*. 2024;45(3):211–223. doi:10.1016/j.it.2024.01.006
11. Stamellou E, Seikrit C, Tang SCW, et al. IgA nephropathy. *Nat Rev Dis Primers*. 2023;9(1):67. doi:10.1038/s41572-023-00476-9
12. Zhang SL, Mao YQ, Zhang ZY, et al. Pectin supplement significantly enhanced the anti-PD-1 efficacy in tumor-bearing mice humanized with gut microbiota from patients with colorectal cancer. *Theranostics*. 2021;11(9):4155–4170. doi:10.7150/thno.54476
13. Nagaishi T, Watabe T, Kotake K, et al. Immunoglobulin A-specific deficiency induces spontaneous inflammation specifically in the ileum. *Gut*. 2022;71(3):487–496. doi:10.1136/gutjnl-2020-322873
14. Zhu Y, He H, Sun W, et al. IgA nephropathy: gut microbiome regulates the production of hypoglycosilated IgA1via the TLR4 signaling pathway. *Nephrol Dial Transplant*. 2024;39(10):1624–1641. doi:10.1093/ndt/gfae052
15. Serafini N, Jarade A, Surace L, et al. Trained ILC3 responses promote intestinal defense. *Science*. 2022;375(6583):859–863. doi:10.1126/science.aaz8777
16. De Angelis M, Montemurno E, Piccolo M, et al. Microbiota and metabolome associated with immunoglobulin A nephropathy (IgAN). *PLoS One*. 2014;9(6):e99006. doi:10.1371/journal.pone.0099006
17. Gao L, Li H, Liu X, et al. Humoral immune responses primed by the alteration of gut microbiota were associated with galactose-deficient IgA1 production in IgA nephropathy. *Front Immunol*. 2024;15:1415026. doi:10.3389/fimmu.2024.1415026
18. Currie EG, Coburn B, Porfilio EA, et al. Immunoglobulin A nephropathy is characterized by anticommensal humoral immune responses. *JCI Insight*. 2022;7(5). doi:10.1172/jci.insight.141289

19. Piccolo M, De Angelis M, Lauriero G, et al. Salivary microbiota associated with immunoglobulin a nephropathy. *Microb Ecol*. 2015;70(2):557–565. doi:10.1007/s00248-015-0592-9
20. Zhao J, Bai M, Ning X, et al. Expansion of Escherichia-Shigella in Gut is associated with the onset and response to immunosuppressive therapy of IgA nephropathy. *J Am Soc Nephrol*. 2022;33(12):2276–2292. doi:10.1681/ASN.2022020189
21. Higashiyama M, Haniuda K, Nihei Y, et al. Oral bacteria induce IgA autoantibodies against a mesangial protein in IgA nephropathy model mice. *Life Sci Alliance*. 2024;7(4):e202402588. doi:10.26508/lsa.202402588
22. Chemouny JM, Gleeson PJ, Abbad L, et al. Modulation of the microbiota by oral antibiotics treats immunoglobulin A nephropathy in humanized mice. *Nephrol Dial Transplant*. 2019;34(7):1135–1144. doi:10.1093/ndt/gfy323
23. Kiryluk K, Li Y, Scolari F, et al. Discovery of new risk loci for IgA nephropathy implicates genes involved in immunity against intestinal pathogens. *Nat Genet*. 2014;46(11):1187–1196. doi:10.1038/ng.3118
24. Yu XQ, Li M, Zhang H, et al. A genome-wide association study in Han Chinese identifies multiple susceptibility loci for IgA nephropathy. *Nat Genet*. 2011;44(2):178–182. doi:10.1038/ng.1047
25. Nagy J, Scott H, Brandtzaeg P. Antibodies to dietary antigens in IgA nephropathy. *Clin Nephrol*. 1988;29(6):275–279.
26. Floege J, Feehally J. The mucosa-kidney axis in IgA nephropathy. *Nat Rev Nephrol*. 2016;12(3):147–156. doi:10.1038/nrneph.2015.208
27. Sallustio F, Curci C, Chaoul N, et al. High levels of gut-homing immunoglobulin A+ B lymphocytes support the pathogenic role of intestinal mucosal hyperresponsiveness in immunoglobulin A nephropathy patients. *Nephrol Dial Transplant*. 2021;36(3):452–464. doi:10.1093/ndt/gfaa264
28. Netea MG, Quintin J, van der Meer JW. Trained immunity: a memory for innate host defense. *Cell Host Microbe*. 2011;9(5):355–361. doi:10.1016/j.chom.2011.04.006
29. Netea MG, Joosten LA, Latz E, et al. Trained immunity: a program of innate immune memory in health and disease. *Science*. 2016;352(6284):aaf1098. doi:10.1126/science.aaf1098
30. Spencer J, Bemark M. Human intestinal B cells in inflammatory diseases. *Nat Rev Gastroenterol Hepatol*. 2023;20(4):254–265. doi:10.1038/s41575-023-00755-6
31. Gutzeit C, Magri G, Cerutti A. Intestinal IgA production and its role in host-microbe interaction. *Immunol Rev*. 2014;260(1):76–85. doi:10.1111/imr.12189
32. Harabuchi Y, Takahara M. Recent advances in the immunological understanding of association between tonsil and immunoglobulin A nephropathy as a tonsil-induced autoimmune/inflammatory syndrome. *Immun Inflamm Dis*. 2019;7(2):86–93. doi:10.1002/iid3.248
33. Pohjonen J, Kaukinen K, Huhtala H, et al. Indirect markers of intestinal damage in IgA nephropathy. *Nephron*. 2024;148(10):693–700. doi:10.1159/000538242
34. Honkanen T, Mustonen J, Kainulainen H, et al. Small bowel cyclooxygenase 2 (COX-2) expression in patients with IgA nephropathy. *Kidney Int*. 2005;67(6):2187–2195. doi:10.1111/j.1523-1755.2005.00324.x
35. Wculek SK, Cueto FJ, Mujal AM, Melero I, Krummel MF, Sancho D. Dendritic cells in cancer immunology and immunotherapy. *Nat Rev Immunol*. 2020;20(1):7–24. doi:10.1038/s41577-019-0210-z
36. Chen S, Saeed A, Liu Q, et al. Macrophages in immunoregulation and therapeutics. *Signal Transduct Target Ther*. 2023;8(1):207. doi:10.1038/s41392-023-01452-1
37. Lafayette R, Kristensen J, Stone A, et al. Efficacy and safety of a targeted-release formulation of budesonide in patients with primary IgA nephropathy (NefIgArd): 2-year results from a randomised Phase 3 trial. *Lancet*. 2023;402(10405):859–870. doi:10.1016/S0140-6736(23)01554-4
38. Smerud HK, Barany P, Lindstrom K, et al. New treatment for IgA nephropathy: enteric budesonide targeted to the ileocecal region ameliorates proteinuria. *Nephrol Dial Transplant*. 2011;26(10):3237–3242. doi:10.1093/ndt/gfr052
39. Zhang H, Lafayette R, Wang B, et al. Efficacy and safety of nefecon in patients with IgA nephropathy from Mainland China: 2-year NefIgArd trial results. *Kidney360*. 2024;5(12):1881–1892. doi:10.34067/KID.0000000583